A study of B^0–$\overline{B}^0$ mixing using semileptonic decays of B hadrons produced from Z^0

DELPHI Collaboration

P. Abreu [a], W. Adam [b], T. Adye [c], E. Agasi [d], R. Aleksan [e], G.D. Alekseev [f], A. Algeri [g], P. Allen [h], S. Almehed [i], S.J. Alvsvaag [j], U. Amaldi [b], E.G. Anassontzis [k], A. Andreazza [ℓ], P. Antilogus [m], W.-D. Apel [n], R.J. Apsimon [c], Y. Arnoud [e], B. Åsman [o], J.-E. Augustin [p], A. Augustinus [d], P. Baillon [b], P. Bambade [p], F. Barao [a], R. Barate [q], G. Barbiellini [r], D.Y. Bardin [f], G. Barker [s], A. Baroncelli [t], O. Barring [i], J.A. Barrio [u], W. Bartl [v], M.J. Bates [c], M. Battaglia [g], M. Baubillier [w], K.-H. Becks [x], C.J. Beeston [s], M. Begalli [y], P. Beilliere [z], Yu. Belokopytov [aa], P. Beltran [ab], D. Benedic [ac], A.C. Benvenuti [ad], M. Berggren [p], D. Bertrand [ae], F. Bianchi [af], M.S. Bilenky [f], P. Billoir [w], J. Bjarne [i], D. Bloch [ac], S. Blyth [s], V. Bocci [ag], P.N. Bogolubov [f], T. Bolognese [e], M. Bonesini [ℓ], W. Bonivento [ℓ], P.S.L. Booth [ah], G. Borisov [aa], H. Borner [b], C. Bosio [t], B. Bostjancic [ai], S. Bosworth [s], O. Botner [aj], E. Boudinov [aa], B. Bouquet [p], C. Bourdarios [p], T.J.V. Bowcock [ah], M. Bozzo [ak], S. Braibant [ae], P. Branchini [t], K.D. Brand [aℓ], R.A. Brenner [b], H. Briand [w], C. Bricman [ae], R.C.A. Brown [b], N. Brummer [d], J.-M. Brunet [z], L. Bugge [am], T. Buran [am], H. Burmeister [b], J.A.M.A. Buytaert [b], M. Caccia [b], M. Calvi [ℓ], A.J. Camacho Rozas [an], R. Campion [ah], T. Camporesi [b], V. Canale [ag], F. Cao [ae], F. Carena [b], L. Carroll [ah], C. Caso [ak], M.V. Castillo Gimenez [h], A. Cattai [b], F.R. Cavallo [ad], L. Cerrito [ag], V. Chabaud [b], A. Chan [ao], Ph. Charpentier [b], L. Chaussard [p], J. Chauveau [w], P. Checchia [aℓ], G.A. Chelkov [f], L. Chevalier [e], P. Chliapnikov [aa], V. Chorowicz [w], J.T.M. Chrin [h], M.P. Clara [af], P. Collins [s], J.L. Contreras [u], R. Contri [ak], E. Cortina [h], G. Cosme [p], F. Couchot [p], H.B. Crawley [ao], D. Crennell [c], G. Crosetti [ak], M. Crozon [z], J. Cuevas Maestro [an], S. Czellar [g], E. Dahl-Jensen [ap], B. Dalmagne [p], M. Dam [am], G. Damgaard [ap], G. Darbo [ak], E. Daubie [ae], A. Daum [n], P.D. Dauncey [s], M. Davenport [b], P. David [w], J. Davies [ah], W. Da Silva [w], C. Defoix [z], D. Delikaris [b], S. Delorme [b], P. Delpierre [z], N. Demaria [af], A. De Angelis [r], H. De Boeck [ae], W. De Boer [n], C. De Clercq [ae], M.D.M. De Fez Laso [h], N. De Groot [d], C. De La Vaissiere [w], B. De Lotto [r], A. De Min [ℓ], H. Dijkstra [b], L. Di Ciaccio [ag], F. Djama [ac], J. Dolbeau [z], M. Donszelmann [b], K. Doroba [aq], M. Dracos [b], J. Drees [x], M. Dris [ar], Y. Dufour [z], F. Dupont [q], L.-O. Eek [aj], P.A.-M. Eerola [b], R. Ehret [n], T. Ekelof [aj], G. Ekspong [o], A. Elliot Peisert [aℓ], J.-P. Engel [ac], N. Ershaidat [w], D. Fassouliotis [ar], M. Feindt [b], M. Fernandez Alonso [an], A. Ferrer [h], T.A. Filippas [ar], A. Firestone [ao], H. Foeth [b], E. Fokitis [ar], F. Fontanelli [ak], K.A.J. Forbes [ah], J.-L. Fousset [as], S. Francon [m], B. Franek [c], P. Frenkiel [z], D.C. Fries [n], A.G. Frodesen [j], R. Fruhwirth [v], F. Fulda-Quenzer [p], K. Furnival [ah], H. Furstenau [n], J. Fuster [b], D. Gamba [af], C. Garcia [h], J. Garcia [an], C. Gaspar [b], U. Gasparini [aℓ], Ph. Gavillet [b], E.N. Gazis [ar], J.-P. Gerber [ac], P. Giacomelli [b], R. Gokieli [aq], B. Golob [ai], V.M. Golovatyuk [f], J.J. Gomez Y Cadenas [b], A. Goobar [o], G. Gopal [c], M. Gorski [aq], V. Gracco [ak], A. Grant [b], F. Grard [ae], E. Graziani [t], G. Grosdidier [p], E. Gross [b], P. Grosse-Wiesmann [b], B. Grossetete [w], S. Gumenyuk [aa], J. Guy [c], U. Haedinger [n], F. Hahn [x], M. Hahn [n], S. Haider [d], A. Hakansson [i], A. Hallgren [aj], K. Hamacher [x], G. Hamel De Monchenault [e], W. Hao [d], F.J. Harris [s], T. Henkes [b], J.J. Hernandez [h], P. Herquet [ae], H. Herr [b], T.L. Hessing [ah], I. Hietanen [g], C.O. Higgins [ah],

E. Higon [h], H.J. Hilke [b], S.D. Hodgson [s], T. Hofmokl [aq], R. Holmes [ao], S.-O. Holmgren [o],
D. Holthuizen [d], P.F. Honore [z], J.E. Hooper [ap], M. Houlden [ah], J. Hrubec [v], K. Huet [ae],
P.O. Hulth [o], K. Hultqvist [o], P. Ioannou [k], D. Isenhower [b], P.-S. Iversen [j], J.N. Jackson [ah],
P. Jalocha [at], G. Jarlskog [i], P. Jarry [e], B. Jean-Marie [p], E.K. Johansson [o], D. Johnson [ah],
M. Jonker [b], L. Jonsson [i], P. Juillot [ac], G. Kalkanis [k], G. Kalmus [c], F. Kapusta [w], M. Karlsson [b],
E. Karvelas [ab], S. Katsanevas [k], E.C. Katsoufis [ar], R. Keranen [g], J. Kesteman [ae], B.A. Khomenko [f],
N.N. Khovanski [f], B. King [ah], N.J. Kjaer [b], H. Klein [b], W. Klempt [b], A. Klovning [j], P. Kluit [d],
A. Koch-Mehrin [x], J.H. Koehne [n], B. Koene [d], P. Kokkinias [ab], M. Kopf [n], A.V. Korytov [f],
V. Kostioukhine [aa], C. Kourkoumelis [k], O. Kouznetsov [f], P.H. Kramer [x], J. Krolikowski [aq],
I. Kronkvist [i], U. Kruener-Marquis [x], W. Krupinski [at], K. Kulka [aj], K. Kurvinen [g], C. Lacasta [h],
C. Lambropoulos [ab], J.W. Lamsa [ao], L. Lanceri [r], V. Lapin [aa], J.-P. Laugier [e], R. Lauhakangas [g],
G. Leder [v], F. Ledroit [q], R. Leitner [au], Y. Lemoigne [e], J. Lemonne [ae], G. Lenzen [x], V. Lepeltier [p],
T. Lesiak [at], J.M. Levy [ac], E. Lieb [x], D. Liko [v], J. Lindgren [g], R. Lindner [x], A. Lipniacka [aq],
I. Lippi [aℓ], B. Loerstad [i], M. Lokajicek [f], J.G. Loken [s], A. Lopez-Fernandez [b],
M.A. Lopez Aguera [an], M. Los [d], D. Loukas [ab], J.J. Lozano [h], P. Lutz [z], L. Lyons [s],
G. Maehlum [am], J. Maillard [z], A. Maltezos [ab], F. Mandl [v], J. Marco [an], M. Margoni [aℓ],
J.-C. Marin [b], A. Markou [ab], T. Maron [x], S. Marti [h], L. Mathis [ao], F. Matorras [an], C. Matteuzzi [ℓ],
G. Matthiae [ag], M. Mazzucato [aℓ], M. Mc Cubbin [ah], R. Mc Kay [ao], R. Mc Nulty [ah], G. Meola [ak],
C. Meroni [ℓ], W.T. Meyer [ao], M. Michelotto [aℓ], I. Mikulec [v], L. Mirabito [m], W.A. Mitaroff [v],
G.V. Mitselmakher [f], U. Mjoernmark [i], T. Moa [o], R. Moeller [ap], K. Moenig [b], M.R. Monge [ak],
P. Morettini [ak], H. Mueller [n], W.J. Murray [c], B. Muryn [at], G. Myatt [s], F.L. Navarria [ad], P. Negri [ℓ],
B.S. Nielsen [ap], B. Nijjhar [ah], V. Nikolaenko [aa], P.E.S. Nilsen [j], P. Niss [o], V. Obraztsov [aa],
A.G. Olshevski [f], R. Orava [g], A. Ostankov [aa], K. Osterberg [g], A. Ouraou [e], M. Paganoni [ℓ],
R. Pain [w], H. Palka [d], Th.D. Papadopoulou [ar], L. Pape [b], A. Passeri [t], M. Pegoraro [aℓ],
J. Pennanen [g], V. Perevozchikov [aa], H. Pernegger [v], M. Pernicka [v], A. Perrotta [ad], C. Petridou [r],
A. Petrolini [ak], L. Petrovykh [aa], T.E. Pettersen [aℓ], F. Pierre [e], M. Pimenta [a], O. Pingot [ae],
S. Plaszczynski [p], M.E. Pol [b], G. Polok [at], P. Poropat [r], P. Privitera [n], A. Pullia [ℓ], D. Radojicic [s],
S. Ragazzi [ℓ], H. Rahmani [ar], P.N. Ratoff [av], A.L. Read [am], N.G. Redaelli [ℓ], M. Regler [v],
D. Reid [ah], P.B. Renton [s], L.K. Resvanis [k], F. Richard [p], M. Richardson [ah], J. Ridky [aw],
G. Rinaudo [af], I. Roditi [ay], A. Romero [af], I. Roncagliolo [ak], P. Ronchese [aℓ], C. Ronnqvist [g],
E.I. Rosenberg [ao], S. Rossi [b], U. Rossi [ad], E. Rosso [b], P. Roudeau [p], T. Rovelli [ad], W. Ruckstuhl [d],
V. Ruhlmann-Kleider [e], A. Ruiz [an], K. Rybicki [at], H. Saarikko [g], Y. Sacquin [e], G. Sajot [q], J. Salt [h],
J. Sanchez [u], M. Sannino [ak], S. Schael [n], H. Schneider [n], B. Schulze [ag], M.A.E. Schyns [x],
G. Sciolla [af], F. Scuri [r], A.M. Segar [s], R. Sekulin [c], M. Sessa [r], G. Sette [ak], R. Seufert [n],
R.C. Shellard [y], I. Siccama [d], P. Siegrist [e], S. Simonetti [ak], F. Simonetto [aℓ], A.N. Sisakian [f],
G. Skjevling [am], G. Smadja [e,m], G.R. Smith [c], R. Sosnowski [b], D. Souza-Santos [y], T.S. Spassoff [q],
E. Spiriti [t], S. Squarcia [ak], H. Staeck [x], C. Stanescu [t], S. Stapnes [am], G. Stavropoulos [ab],
F. Stichelbaut [ae], A. Stocchi [p], J. Strauss [v], J. Straver [b], R. Strub [ac], B. Stugu [j], M. Szczekowski [b],
M. Szeptycka [aq], P. Szymanski [aq], T. Tabarelli [ℓ], O. Tchikilev [aa], G.E. Theodosiou [ab],
A. Tilquin [as], J. Timmermans [d], V.G. Timofeev [f], L.G. Tkatchev [f], T. Todorov [ac], D.Z. Toet [d],
O. Toker [g], E. Torassa [af], L. Tortora [t], D. Treille [b], U. Trevisan [ak], W. Trischuk [b], G. Tristram [z],
C. Troncon [ℓ], A. Tsirou [b], E.N. Tsyganov [f], M. Turala [at], M.-L. Turluer [e], T. Tuuva [g],
I.A. Tyapkin [w], M. Tyndel [c], S. Tzamarias [b], S. Ueberschaer [x], O. Ullaland [b], V. Uvarov [aa],
G. Valenti [ad], E. Vallazza [af], J.A. Valls Ferrer [h], C. Vander Velde [ae], G.W. Van Apeldoorn [d],
P. Van Dam [d], M. Van Der Heijden [d], W.K. Van Doninck [ae], P. Vaz [b], G. Vegni [ℓ], L. Ventura [aℓ],
W. Venus [c], F. Verbeure [ae], L.S. Vertogradov [f], D. Vilanova [e], P. Vincent [m], L. Vitale [g],
E. Vlasov [aa], A.S. Vodopyanov [f], M. Vollmer [x], G. Voulgaris [k], M. Voutilainen [g], V. Vrba [t],

H. Wahlen[x], C. Walck[o], F. Waldner[r], M. Wayne[ao], A. Wehr[x], M. Weierstall[x], P. Weilhammer[b], J. Werner[x], A.M. Wetherell[b], J.H. Wickens[ae], G.R. Wilkinson[s], W.S.C. Williams[s], M. Winter[ac], M. Witek[at], G. Wormser[p], K. Woschnagg[aj], N. Yamdagni[o], P. Yepes[b], A. Zaitsev[aa], A. Zalewska[at], P. Zalewski[p], D. Zavrtanik[ai], E. Zevgolatakos[ab], G. Zhang[x], N.I. Zimin[f], M. Zito[e], R. Zuberi[s], R. Zukanovich Funchal[z], G. Zumerle[aℓ] and J. Zuniga[h]

[a] *LIP, IST, FOUL, Av. Elias Garcia 14-1o, P-1000 Lisbon Codex, Portugal*
[b] *CERN, CH-1211 Geneva 23, Switzerland*
[c] *Rutherford Appleton Laboratory, Chilton, Didcot OX11 0QX, UK*
[d] *NIKHEF-H, Postbus 41882, NL-1009 DB Amsterdam, The Netherlands*
[e] *DSM/DAPNIA, Centre d'Etude de Saclay, F-91191 Gif-sur-Yvette Cedex, France*
[f] *Joint Institute for Nuclear Research, Dubna, Head Post Office, P.O. Box 79, 101 000 Moscow, Russian Federation*
[g] *Research Institute for High Energy Physics, University of Helsinki,*
   Siltavuorenpenger 20 C, SF-00170 Helsinki 17, Finland
[h] *IFIC, Valencia–CSIC, and DFAMN, Universidad de Valencia,*
   Avda. Dr. Moliner 50, E-46100 Burjassot (Valencia), Spain
[i] *Department of Physics, University of Lund, Sölvegatan 14, S-22363 Lund, Sweden*
[j] *Department of Physics, University of Bergen, Allégaten 55, N-5007 Bergen, Norway*
[k] *Physics Laboratory, University of Athens, Solonos Street 104, GR-10680 Athens, Greece*
[ℓ] *Dipartimento di Fisica, Università di Milano and INFN, Via Celoria 16, I-20133 Milan, Italy*
[m] *IPNL, Université Claude Bernard de Lyon, IN2P3-CNRS, F-69622 Villeurbanne Cedex, France*
[n] *Institut für Experimentelle Kernphysik, Universität Karlsruhe, Pf. 6980, W-7500 Karlsruhe 1, FRG*
[o] *Institute of Physics, University of Stockholm, Vanadisvägen 9, S-113 46 Stockholm, Sweden*
[p] *Laboratoire de l'Accélérateur Linéaire, IN2P3-CNRS, Université de Paris-Sud, Bâtiment 200, F-91405 Orsay, France*
[q] *Institut des Sciences Nucléaires, Université de Grenoble 1, F-38026 Grenoble, France*
[r] *Dipartimento di Fisica, Università di Trieste and INFN, Via A. Valerio 2, I-34127 Trieste, Italy*
   and Istituto di Fisica, Università di Udine, I-33100 Udine, Italy
[s] *Nuclear Physics Laboratory, University of Oxford, Keble Road, Oxford OX1 3RH, UK*
[t] *Istituto Nazionale di Fisica Nucleare (INFN),Istituto Superiore di Sanità, Viale Regina Elena 299, I-00161 Rome, Italy*
[u] *Universidad Complutense, Avda. Complutense s/n, E-28040 Madrid, Spain*
[v] *Institut für Hochenergiephysik, Österreichische Akademie der Wissenschaften,*
   Nikolsdorfergasse 18, A-1050 Vienna, Austria
[w] *LPNHE, Universités Paris VI et VII, Tour 33 (RdC), 4 place Jussieu, F-75252 Paris Cedex 05, France*
[x] *Fachbereich Physik, University of Wuppertal, Pf. 100 127, W-5600 Wuppertal 1, FRG*
[y] *Departamento de Fisica, Pontificia Universidade Católica, CP 38071 RJ-22453 Rio de Janeiro, Brazil*
[z] *Laboratoire de Physique Corpusculaire, IN2P3-CNRS, Collège de France, F-75231 Paris Cedex 5, France*
[aa] *Institute for High Energy Physics, Serpukhov, P.O. Box 35, 142 284 Protvino (Moscow Region), Russian Federation*
[ab] *Institute of Nuclear Physics, NCSR Demokritos, P.O. Box 60228, GR-15310 Athens, Greece*
[ac] *Centre de Rercherche Nucléaire, IN2P3-CNRS/ULP-B.P. 20, F-67037 Strasbourg Cedex, France*
[ad] *Dipartimento di Fisica, Università di Bologna and INFN, Via Irnerio 46, I-40126 Bologna, Italy*
[ae] *Physics Department, Universitaire Instelling Antwerpen, Universiteitsplein 1, B-2610 Wilrijk, Belgium*
   and IIHE, ULB–VUB, Pleinlaan 2, B-1050 Brussels, Belgium
   and Faculté des Sciences, Université de l'Etat Mons, Av. Maistriau 19, B-7000 Mons, Belgium
[af] *Dipartimento di Fisica Sperimentale, Università di Torino and INFN, Via P. Giuria 1, I-10125 Turin, Italy*
[ag] *Dipartimento di Fisica, Università di Roma II and INFN, Tor Vergata, I-00173 Rome, Italy*
[ah] *Department of Physics, University of Liverpool, P.O. Box 147, Liverpool L69 3BX, UK*
[ai] *J. Stefan Institute and Department of Physics, University of Ljubljana, Jamova 39, SI-61000 Ljubljana, Slovenia*
[aj] *Department of Radiation Sciences, University of Uppsala, P.O. Box 535, S-751 21 Uppsala, Sweden*
[ak] *Dipartimento di Fisica, Università di Genova and INFN, Via Dodecaneso 33, I-16146 Genoa, Italy*
[aℓ] *Dipartimento di Fisica, Università di Padova and INFN, Via Marzolo 8, I-35131 Padua, Italy*
[am] *Physics Department, University of Oslo, Blindern, N-1000 Oslo 3, Norway*
[an] *Facultad de Ciencias, Universidad de Santander, av. de los Castros, E-39005 Santander, Spain*
[ao] *Ames Laboratory and Department of Physics, Iowa State University, Ames IA 50011, USA*
[ap] *Niels Bohr Institute, Blegdamsvej 17, DK-2100 Copenhagen Ø, Denmark*
[aq] *Institute for Nuclear Studies, and University of Warsaw, Ul. Hoża 69, PL-00681 Warsaw, Poland*
[ar] *Physics Department, National Technical University, Zografou Campus, GR-15773 Athens, Greece*

^{as} *CPP, Université d'Aix, Marseille II, IN2P3-CNRS, F-13288 Marseille Cedex 09, France*
^{at} *High Energy Physics Laboratory, Institute of Nuclear Physics, Ul. Kawiory 26 a, PL-30055 Cracow 30, Poland*
^{au} *NC, Nuclear Centre of MFF, Charles University, Areal MFF, V Holesovickach 2, 180 00, Prague 8, Czech Republic*
^{av} *School of Physics and Materials, University of Lancaster, Lancaster LA1 4YB, UK*
^{aw} *FZU, Institute of Physics of the C.A.S. High Energy Physics Division, Na Slovance 2, 180 40, Prague 8, Czech Republic*
^{ay} *Centro Brasileiro de Pesquisas Fisicas, rua Xavier Sigaud 150, RJ-22290 Rio de Janeiro, Brazil*

The B^0-$\overline{B}^0$ mixing was studied by using about 250 000 hadronic decays of the Z^0, collected with the DELPHI detector at LEP. With 1665 dilepton events, the probability for a b quark to become a $\bar{b}$ before decaying was found to be $\chi = 0.121^{+0.044}_{-0.040} \pm 0.017$. The semileptonic branching ratio of the b was measured from the dilepton and single lepton events and found to be $\text{Br}(b \rightarrow \ell) = (10.0 \pm 0.7 \pm 0.7)\%$.

1. Introduction

Several measurements of the B^0-$\overline{B}^0$ mixing probability have already been published from experiments at LEP [1], at other e^+e^- machines and at hadron colliders [2].

At LEP, in the decays $Z^0 \rightarrow b\bar{b}$, both B^0_s and B^0_d mesons are produced, as well as charged B-mesons and b-flavoured baryons which do not mix. Therefore, the measured mixing is an average. In this letter, the semileptonic decays of B-hadrons have been used to measure the average mixing parameter χ,

$$\chi = \frac{b \rightarrow \overline{B}^0 \rightarrow B^0 \rightarrow \ell^+}{b \rightarrow \ell^\pm}. \qquad (1)$$

The measured χ is

$$\chi = f_d \chi_d + f_s \chi_s, \qquad (2)$$

where f_d and f_s are the fractions of leptons arising from B^0_d and B^0_s decays, and χ_d and χ_s are the mixing parameters of B^0_d and B^0_s mesons, respectively.

Box diagrams lead to mixing of B^0 and $\overline{B}^0$ in the same way as in the K^0-$\overline{K}^0$ system. The rate of mixing depends on the top quark mass and on the elements V_{td} and V_{ts} of the Cabibbo-Kobayashi-Maskawa matrix.

In the analysis described in this letter, events of the type $Z^0 \rightarrow q\bar{q} \rightarrow$ hadrons were used, with two identified leptons, either electrons or muons, in the final state. The signal consists of dilepton events, with both leptons coming from direct b decay and being of the same charge (henceforth called PB–PB). Other possible origins of like sign dilepton events are:

– events in which both leptons are from $b \rightarrow c \rightarrow \ell$ (secondary $c = SC$). These events are sensitive to the mixing parameter in the same way as when both leptons are from primary b parents. This configuration will be called SC–SC in the following.
– $b \rightarrow c \rightarrow \ell$ (SC) together with $\bar{b} \rightarrow \ell$ (primary $b = PB$) is sensitive to the mixing in the opposite way, i.e. the fraction of opposite sign dilepton events is proportional to the mixing. This configuration will be referred to as PB–SC.
– a misidentified hadron together with a lepton of the same sign from a semileptonic decay of a heavy quark, or two misidentified hadrons of the same sign. This configuration will be referred to as BKG-any.

Events originating from $c\bar{c}$, where both c quarks decay semileptonically, contribute only to the opposite charge dilepton events, and will be referred to as PC–PC.

2. Event sample and lepton identification

The data described in this letter were taken with the DELPHI detector at LEP. The detector has been described elsewhere [3]. The parts of the detector relevant for this analysis were: the central tracking system consisting of the Time Projection Chamber (TPC), the inner and outer detectors (ID and OD), which measures momenta with a resolution of 8% at 45 GeV/c; the electromagnetic calorimeter, HPC, which was used to identify electrons, and covers the central region $|\cos\theta| < 0.7$, where θ is the polar angle with respect to the beam direction; and the muon chambers covering the regions $|\cos\theta| < 0.6$ and $0.7 <$

$|\cos\theta| < 0.93$. In addition, TPC, which covers the angular range $|\cos\theta| < 0.93$, gives up to 192 samples of dE/dx, which were used for electron identification.

Both charged and neutral particles were used in the event reconstruction. Hadronic decays $Z^0 \to q\bar{q}$ were selected by requiring at least 7 charged particle tracks. Tracks were selected if they had an impact parameter to the nominal interaction vertex below 5 cm in the transverse plane with respect to the beam axis, and below 10 cm along the beam direction, and a momentum of at least 200 MeV/c. A neutral particle was accepted, if the deposited energy in the electromagnetic calorimeter was larger than 0.7 GeV. Events were accepted only if the total visible energy was larger than $0.3 \times E_{cm}$ and if the relevant detector parts used for this analysis, i.e. TPC, HPC and the muon chambers, were fully operational.

This gave 112 700 events from the 1991 run and 59 450 from the 1990 run with the thrust axis in the region $|\cos\theta_T| < 0.65$, where there is a high efficiency to identify both muons and electrons, and 76 846 events from the 1991 running with $0.65 < |\cos\theta_T| < 0.90$, where only the muon identification could be used.

In each event, a cluster analysis was made with the LUND algorithm LUCLUS [4] using both charged and neutral particles. The transverse momentum p_t of a lepton was defined as the momentum component transverse to the rest of the cluster to which the lepton belonged, after the lepton itself had been removed from the cluster.

The muon identification was performed by combining the muon chamber hits with the tracking information and has been described in detail elsewhere [5]. Only charged particles with momentum larger than 3 GeV/c were considered. The muon candidate must be associated with hits in at least two planes of the muon chambers, one of which must be outside the iron return yoke. The criteria to identify a particle as a muon were based on a χ^2 fit, where the χ^2 was calculated from the difference between the extrapolated track trajectory and the fitted track element constructed from the hits in the muon chambers. The efficiency of the algorithm to identify a muon with these criteria was $(78 \pm 2)\%$ [6].

The electron identification [7] was performed using the ionization loss dE/dx measured in TPC, and the energy and the transverse and longitudinal shape

Table 1
Efficiency to tag an electron in two regions of p_t, determined from the data.

Region p_t (GeV/c)	ϵ_e (%)	P_e (%)
$p_t < 1$ GeV/c	60 ± 2	61 ± 2
$p_t > 1$ GeV/c	73 ± 2	70 ± 2

of the shower measured in HPC, exploiting the detailed granularity of the electromagnetic calorimeter which gives a three-dimensional image of the shower. Electrons were identified in HPC by utilizing a single canonical variable, constructed with the statistical analysis SAS package [8] to determine the weights with which to combine linearly the transverse and longitudinal shower shape variables. This identification algorithm takes into account the energy (E) deposited in the calorimeter, and the extrapolated momentum (p), without the need of an explicit cut on E/p, which is uncertain due to the energy resolution of the gas calorimeter. The identification was applied to charged particles with p larger than 3.5 GeV/c.

The efficiency of electron identification was determined using the dE/dx information to define a sample of electrons and hadrons in the data. The hadron sample was defined as all charged particles with dE/dx less than 1.3, the expected value for a minimum ionizing particle being 1.0. The complementary sample with dE/dx greater than 1.3 is a mixture of hadrons and electrons. The true electron sample was determined statistically by subtracting from this sample the fraction of hadrons, estimated from the sample with dE/dx less than 1.3 weighting appropriately for the different momentum spectra of the samples.

Table 1 gives the electron identification efficiency ϵ_e (in percent) in different regions of p_t, determined from the data, together with the purity P_e, defined as the fraction of true electrons in the selected sample.

For comparison, the efficiency determined from Monte Carlo with full detector simulation for electrons in the region of p_t greater than 1.0 GeV/c was $(78 \pm 2)\%$, and the purity of the sample in the same momentum region was $(77 \pm 2)\%$. The overall hadron misidentification probability was found to be $(0.78 \pm 0.2)\%$ in data and $(0.91 \pm 0.1)\%$ from simulation. Checks were also made with charged particles of

known nature, from K_S^0 decay (charged pions) and γ conversions (electrons). The efficiency for electrons from converted γ or Dalitz pairs was determined to be $(56 \pm 2)\%$ from the 1990 data and $(58 \pm 3)\%$ from simulation. The agreement was also satisfactory for hadron misidentification. The efficiency for identifying leptons is, however, not crucial for measuring the mixing parameter, because the measurement is obtained from the ratio of the number of dilepton events as defined in section 3 below.

The sample defined by the above criteria consisted of 656 $\mu\mu$, 260 ee, and 749 eμ events with the two leptons in opposite hemispheres with respect to a plane perpendicular to the thrust axis. Out of these, 357 were $\ell^+\ell^+$, 366 were $\ell^-\ell^-$ and 942 were $\ell^+\ell^-$ topology. In addition, there were 789 events with two leptons in the same hemisphere. If there were three leptons found in the event, the two leptons with highest p_t were considered in the analysis.

3. Analysis method

To estimate the composition of the dilepton sample, about 320 000 simulated $q\bar{q}$ events were used. The events were generated by using the Lund Parton Shower (PS) model in the JETSET 7.2 program [4], passed through the full detector simulation, and processed with the same event reconstruction as the data. A special Monte Carlo sample of 21 000 $b\bar{b} \rightarrow \ell\ell + X$ events (with leptons from $b \rightarrow \ell$ and $b \rightarrow c \rightarrow \ell$ decays), generated with the PS model and treated in the same way as the simulated $q\bar{q}$ events, was also used. The total statistics of simulated events corresponds to nearly 1 million hadronic decays of the Z^0.

The fragmentation process was described by the string scheme using the Lund left–right symmetric fragmentation function [9] with parameters tuned to describe DELPHI data [10]. The branching ratios were set to 10% for $b \rightarrow \ell$, 10% for $c \rightarrow \ell$, and 20% for $b \rightarrow D^{**}$. One percent of b decays occurred through the channel $b \rightarrow \bar{c} \rightarrow \ell$.

Background to the muon sample originates from punch through hadrons, misassociations of hits in the muon chambers, and hadron decays. For electrons, background is generated by γ conversions (the material in front of the HPC calorimeter corresponds to 0.7 radiation lengths on the average), and hadrons

Table 2
Opposite jet dilepton sample composition from the simulation ($p_t > 1$ GeV/c). The values are in percent.

Composition	$\mu\mu$	ee	eμ	all
PB–PB	53 ± 3	56 ± 5	50 ± 4	52 ± 2
PB–SC	23 ± 3	19 ± 4	16 ± 2	19 ± 2
SC–SC	1 ± 1	3 ± 2	1 ± 1	1 ± 1
PC–PC	2 ± 1	2 ± 1	2 ± 1	2 ± 1
BKG–any	21 ± 3	20 ± 4	31 ± 3	26 ± 2

misidentified as electrons. Conversions and Dalitz pairs were rejected with an efficiency of $(37 \pm 1)\%$ by requiring that the minimum invariant mass with a particle of opposite charge was larger than 150 MeV/c^2.

Table 2 shows the composition of the selected simulated sample of dileptons in opposite jets, when both leptons have a p_t larger than 1 GeV/c.

The semileptonic b decays are expected to produce leptons with high p and p_t. In fig. 1, the distributions of p and p_t for all leptons in events with leptons in opposite jets are compared to those expected from the different sources of dileptons identified in the simulation. In fig. 2, the same quantities are compared for leptons in the same jet. It is clearly seen, that the simulation predicts and describes quite well the momentum distributions of the like sign leptons in the same jet – these events are pure background (figs. 2b and 2d).

To maximize the separation between the signal and the background, two variables were used: the vector product of the momenta of the two leptons $|\boldsymbol{p}_1 \times \boldsymbol{p}_2|$, and the smaller of the p_t values of the two leptons. Fig. 3 shows the scatter plots expected for these variables for the signal and the background separately.

These two variables were combined to define

$$p_{\text{dil}} = \sqrt{\tfrac{1}{16}|\boldsymbol{p}_1 \times \boldsymbol{p}_2| + (p_t^{\text{min}})^2} . \tag{3}$$

Fig. 4 shows the distribution of this variable for data and simulation. In the region p_{dil} greater than 2 GeV/c, the contribution from PB–PB dominates (65%). This region contains 48 dilepton events of the same sign and 106 of opposite sign, giving a mixing parameter $\chi = (11.4^{+4.8}_{4.5})\%$. The value of χ was obtained in this case by comparing the measured ratio of same sign and opposite sign events (R) to
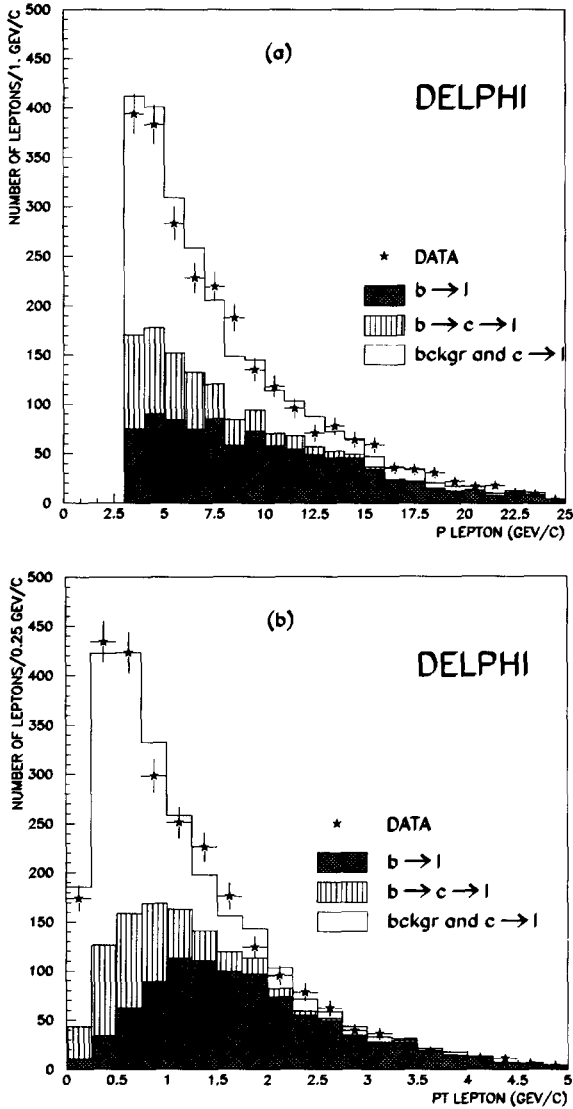
Fig. 1. Leptons in opposite jets: (a) p and (b) p_t distributions of the leptons for the data (stars) and the simulation (histograms). The dark shaded region shows the contribution of leptons from primary b, the vertically hatched region from secondary c, and the white region from background.

the expression of that ratio given by the Monte Carlo simulation expressed as a function of χ.

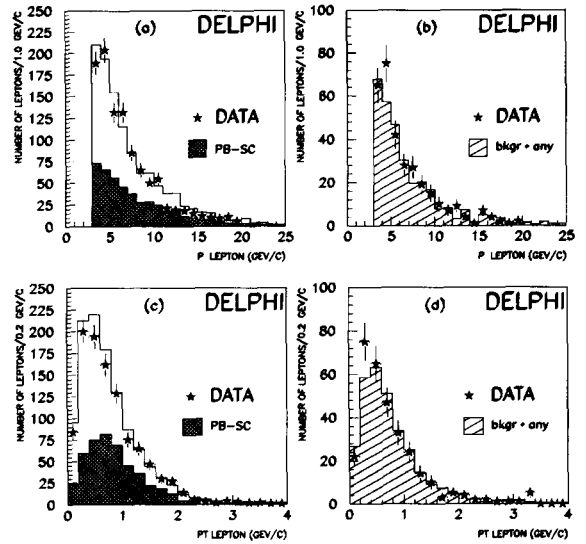## 4. Measurement of χ

Using the full sample of dilepton events, the ratio R,

Fig. 2. Leptons in the same jet: (a) p distributions for the data (stars) and the simulation (histograms) for the opposite charge leptons. The dark shaded region shows the PB–SC contribution. (b) p distributions for the data (stars) and the simulation (histograms) for the same charge leptons. The vertically hatched region is from events with at least one lepton from the background. (c) and (d) show the p_t distributions for the opposite and same charge leptons, respectively.
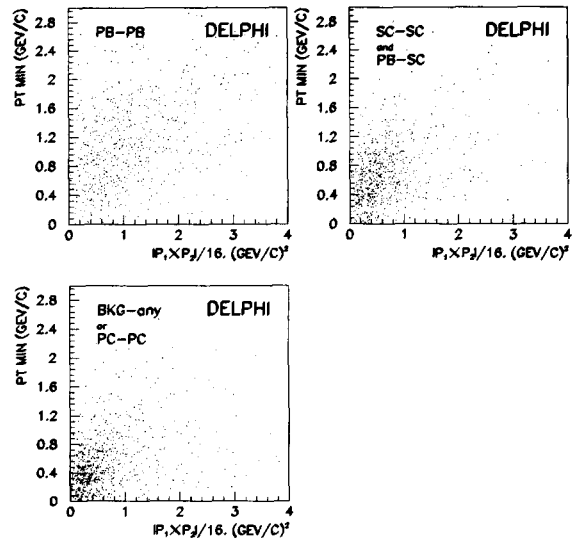

Fig. 3. $|p_1 \times p_2|/16$ versus p_t for leptons from (a) PB–PB, (b) SC–SC and PB–SC and (c) at least one lepton from background.
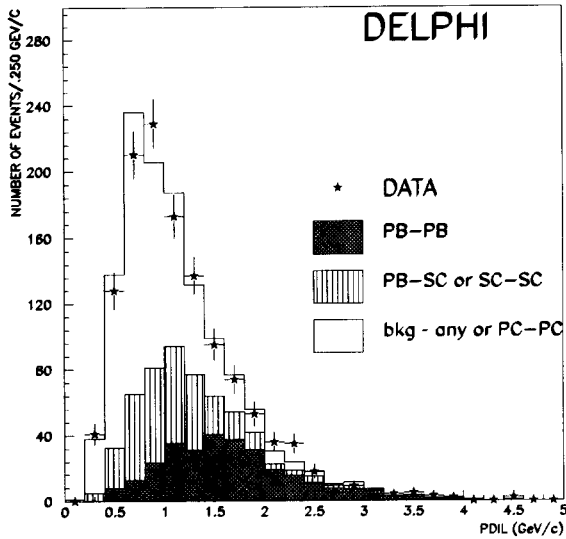
Fig. 4. p_{dil} distribution for the data (stars) and the simulation (histograms). The dark shaded region shows the contribution from PB–PB, the vertically hatched region from PB–SC and SC–SC, and the white region from BKG–any and PC–PC.

$$R = \frac{(\ell^-\ell^-) + (\ell^+\ell^+)}{(\ell^-\ell^+) + (\ell^{\pm}\ell^{\pm})}, \qquad (4)$$

was calculated as a function of p_{dil}, and the mixing parameter χ was fitted from this distribution with the chisquared method.

Possible biases in the measurement due to correlations in the background were investigated with simulation. In a b quark jet, a charged kaon coming directly from the secondary c quark has the same sign as a prompt lepton from b. It was found that 75% of kaons with p greater than 3 GeV/c are correlated in sign with the b quark. The probability that a kaon with p greater than 3 GeV/c is tagged as a muon is 1.7%. Background events with a lepton coming from b and a kaon tagged as a muon behave as signal with respect to the mixing parameter. This effect was taken into account in the fitting procedure. When Monte Carlo events were generated with a fixed value of the χ parameter, the sign of (b $\rightarrow$ ℓK) and (b $\rightarrow$ c $\rightarrow$ ℓK) events were weighted according to the χ parameter and the kaon momentum.

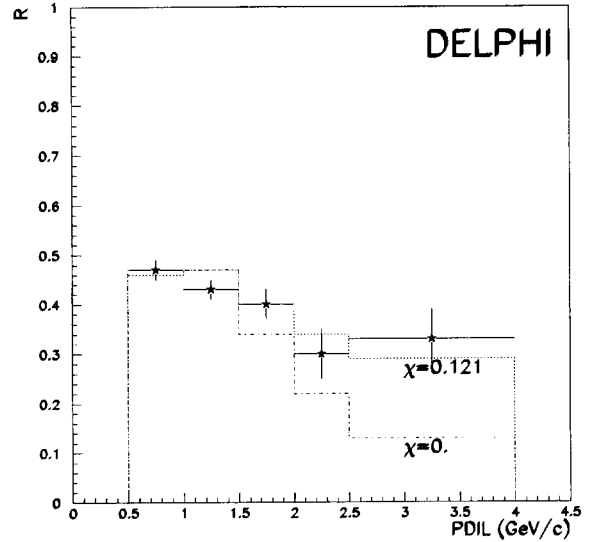The value obtained from the fit was

Fig. 5. Ratio R as a function of p_{dil} together with the fitted values corresponding to $\chi = 0.121$ (dotted line). Also shown (dash-dotted line) are the values corresponding to $\chi = 0$.

$$\chi = (12.1^{+4.4}_{-4.0})\%, \qquad (5)$$

where the error is statistical, but it also takes into account the limited statistics of the Monte Carlo sample used in the fit. Fig. 5 shows the result of the fit compared to the data.

Other variables, like p_t^{min} alone, were also tried to discriminate between the signal and the background. The result obtained from the fit was

$$\chi = (11.5^{+4.5}_{-4.2})\%. \qquad (6)$$

Table 3
Contributions to the systematic uncertainty in the measurement of the mixing parameter. Variations given in percent are relative to the values in the simulation.

Source	Variation	Change in χ
Br(b $\rightarrow$ ℓ)	$\pm10\%$	±0.011
Br(c $\rightarrow$ ℓ)	$\pm10\%$	±0.006
Br(b $\rightarrow$ c)	-3%	$+0.003$
hadron		
misidentification	$\pm20\%$	±0.004
fragmentation		
function	$\langle x_B \rangle = 0.68-0.74$	±0.010

There are several sources of systematic uncertainties intrinsic to the simulation used to estimate the background. The variations taken into account are shown in table 3, together with the effects on χ. $\langle x_B \rangle$ is the mean fraction of energy taken by the B-hadron in the fragmentation process. The total systematic uncertainty in the mixing measurement was obtained by adding in quadrature the contributions, giving $\pm 1.7\%$.

5. Measurement of Br(b → ℓ)

In addition to the mixing measurement, it is possible to extract the average branching ratios of the b quark into electrons and muons from the samples of single and dilepton events.

The branching ratios were obtained from the ratio between the number of events containing two leptons and the total number of leptons observed, with each lepton having p_t greater than 1.0 GeV/c. In this ratio, the Z^0 decay width to the b quark cancels, but one detection efficiency factor for the leptons coming from the b decay remains. This efficiency factor was estimated from simulation. The values used were $(46.6 \pm 1.5)\%$ for muons and $(30.3 \pm 1.1)\%$ for electrons, and they include the efficiency of the algorithm to identify the lepton as well as the cut in the lepton spectra, the efficiency of track reconstruction and the efficiency of associating a track to a shower in the case of electrons. The fraction of leptons coming directly from a b decay was estimated by taking the contributions of leptons other than from direct b decays from the full simulation of DELPHI. The description of the background was checked with the same sign–same jet dilepton events, which are pure background. Figs. 2b and 2d show that the agreement of the simulation with the data is satisfactory. This gives confidence that both the shape and the absolute amount of background estimated for the opposite jet dilepton sample and the single lepton sample are reasonable.

From ee events it was found:

$$\mathrm{Br}(b \to e) = [10.7 \pm 1.5 \ (\text{stat.})]\% . \qquad (7)$$

From $\mu\mu$ events it was found:

$$\mathrm{Br}(b \to \mu) = [11.0 \pm 1.2 \ (\text{stat.})]\% . \qquad (8)$$

The whole sample of ee + $\mu\mu$ + eμ events yielded a

Table 4
Contributions to the systematic uncertainty in the measurement of the semileptonic branching ratios. Variations given in percent are relative to the simulation values.

Source	Variation	Absolute change in Br($b \to \ell$)
Br($c \to \ell$)	$\pm 10\%$	$\pm 0.2\%$
background	$\pm 15\%$	$\pm 0.2\%$
efficiency	$\pm 3\%$	$\pm 0.3\%$
b fragmentation	$\langle x_B \rangle = 0.68$–$0.71$	$\pm 0.4\%$
p_t cut	$p_t > 1.2$ GeV/c	-0.4%

mean branching ratio

$$\mathrm{Br}(b \to \ell) = [10.0 \pm 0.7 \ (\text{stat.})]\% , \qquad (9)$$

where ℓ is a muon or an electron. This measurement can be compared with the value obtained by DELPHI in ref. [11].

Several sources of systematic uncertainties were considered: the Monte Carlo sample composition, the efficiency to identify leptons (which is the most crucial parameter), the b quark fragmentation, and a different interval of p_t in which to perform the measurement. Their effects are reported in table 4. The total systematic uncertainty from these sources is $\pm 0.7\%$.

6. Conclusions

Using a sample of 1665 dilepton events, the average B^0–$\bar{B}^0$ mixing parameter in the Z^0 decays has been found to be

$$\chi = 0.121^{+0.044}_{-0.040} \ (\text{stat.}) \pm 0.017 \ (\text{syst.}) . \qquad (10)$$

The semileptonic branching ratio of B-hadrons, measured from the dilepton and single lepton events, has been found to be

$$\mathrm{Br}(b \to \ell) = [10.0 \pm 0.7 \ (\text{stat.}) \pm 0.7 \ (\text{syst.})]\% , \qquad (11)$$

where ℓ is either a muon or an electron.

References

[1] L3 Collab., B. Adeva et al., Phys. Lett. B 252 (1990) 703;
ALEPH Collab., D. Decamp et al., Phys. Lett B 258 (1991) 236;
OPAL Collab., P.D. Acton et al., Phys. Lett. B 276 (1992) 379.
[2] UA1 Collab., C. Albajar et al., Phys. Lett. B 186 (1987) 247;
MAC Collab., H.R. Band et al., Phys. Lett. B 200 (1988) 221;
CLEO Collab., M. Artuso et al., Phys. Rev. Lett. 62 (1989) 2233;
MARK II Collab., A.J. Weir et al., Phys. Lett. B 240 (1990) 289;
CDF Collab., F. Abe et al., Phys. Rev. Lett. 67 (1991) 3351;
ARGUS Collab., H. Albrecht et al., Z. Phys. C55 (1992) 357.
[3] DELPHI Collab., P. Aarnio et al., Nucl. Instrum. Methods A 303 (1991) 233.
[4] T. Sjöstrand et al., Comput. Phys. Commun. 39 (1986) 347; 43 (1987) 367.
[5] N. Crosland, P. Kluit and G. Wilkinson, Muon identification within DELPHI, DELPHI NOTE 92-17 PHYS 157 (CERN, Geneva, February 1992).
[6] DELPHI Collab., P. Abreu et al., Phys. Lett. B 276 (1992) 536.
[7] M. Calvi, F. Cavallo and C. Matteuzzi, An algorithm to identify electrons using the HPC electromagnetic calorimeter of the DELPHI detector, DELPHI NOTE 91-38 PROG 173 (CERN, Geneva, July 1991).
[8] SAS package, SAS Institute Inc. (Cary, NC, USA).
[9] T. Sjöstrand et al., in: Z physics at LEP 1, Vol. 3, eds. G. Altarelli et al., CERN 89-08 (CERN, Geneva, September 1989).
[10] W. de Boer and H. Furstenau, Invited talk at MC91 (Amsterdam, April 1991), Workshop on Detector and event simulation in high energy physics, eds. K. Bos and B. van Eijk (NIKHEF-H, Amsterdam, 1991).
[11] DELPHI Collab., P. Abreu et al., Z. Phys. C 56 (1992) 47.